Sustainable Energy Technologies and Assessments 48 (2021) 101557

Contents lists available at ScienceDirect

Sustainable Energy Technologies and Assessments

journal homepage: www.elsevier.com/locate/seta

Renewables-polygeneratio

Thermal efficiency analysis of the phase change material (PCM) microcapsules

M. Mazlan [a], M. Rahmani-dehnavi [b], G. Najafi [b,*], B. Ghobadian [b], S.S. Hoseini [b], E. Fayyazi [b], R. Mamat [c], Raslan A. Alenezi [d], M. Mofijur [e]

[a] Faculty of Bioengineering and Technology, Advanced Material Cluster, Universiti Malaysia Kelantan, Jeli, Kelantan, Malaysia
[b] Tarbiat Modares University, Tehran, Iran
[c] School of Mechanical Engineering, Ningxia University, China
[d] Department of Chemical Engineering, College of Technological Studies, Public Authority for Applied Education and Training, PO. Box 42325, Shuwaikh 70654, Kuwait
[e] Centre for Technology in Water and Wastewater, School of Civil and Environmental Engineering, University of Technology Sydney, Ultimo, NSW 2007, Australia

ARTICLE INFO

Keywords:
Thermal energy storage unit
Micro combined heat and power
Phase change material
Paraffin wax
Response surface methodology

ABSTRACT

The aim of the present study is to evaluate the thermal behavior of cylindrical modules in a thermal energy storage unit as a combined sensible and latent heat. A thermal energy storage unit is designed, fabricated, and connected to a cold and hot water supply at constant temperatures to monitor the performance of the storage unit. The thermal energy storage unit contains the cylindrical microcapsules containing paraffin waxes as a phase change material which is located inside an insulating cylinder storage tank. Water is used as a heat transfer fluid to transfer heat from a hot water reservoir to the thermal energy storage unit during the phase change material charging process and also during the discharging process water receives heat from the thermal energy storage unit. Charge tests are carried out at the constant temperature. Moreover, the effect of different inlet flow on storage unit performance is investigated. Data were analyzed using Design Expert software and regression analysis which indicated that the increase of charge inlet temperature and charge inlet flow leads to the increase of heat power, thermal performance of thermal energy storage unit, and output variables. In comparison to the heat storage system without phase change material, microcapsules phase change material can improve the heat power of the heat storage system. Also, based on the optimization process, the maximum thermal performance of 96.4% and the maximum heat power level of 1.7 kW can be achieved in the optimized condition of the charging inlet temperature of 75 °C, charging inlet flow of 1.8^{-4} m^3/s, and discharging inlet temperature of 35 °C.

Introduction

Thermal energy storage (TES) systems, which are actually responsible for storing heat or cold for further use, are used in all places where there is a mismatch between supply and demand for energy [1,2]. In order to achieve sustainable, efficient, and low carbon energy in the construction sector, TES encompasses a range of opportunities and benefits to reduce energy consumption and emissions of greenhouse gases [3,4]. The use of these systems can reduce the amount of CO_2 emissions by %5.5 [5].

Typically, TES systems are divided into types including active and passive systems. Active storage systems include an auxiliary mechanical component for generating heat transfer between the system and the source [6–9]. Therefore, in this type of system, heat transfer will occur as a compulsory displacement. In contrast, in passive systems, the heat transfer between the system and the heat source occurs by the natural convective flow (free movement) or floating forces (due to density difference) without the intervention of any external stimulus [10,11]. Active storage systems are divided by two categories of direct and indirect systems.

Effective ways to improve the efficiency of the TES systems

The effective way to improve the efficiency of the TES systems is using the phase change material (PCM) [12]. Yazdanshenas and Khalesidoost [13] used paraffin to design a thermal reservoir for storing solar energy. The results of this study indicated that the thermal efficiency and solar energy efficiency improved with PCM storage system. In Chu & Choi's [14] study, the thermal variables of the storage system

* Corresponding author at: Tarbiat Modares University, Jalal Ale Ahmad, Nasr, P.O.Box: 14115-111, Tehran, Iran.
E-mail address: g.najafi@modares.ac.ir (G. Najafi).

https://doi.org/10.1016/j.seta.2021.101557
Received 17 October 2020; Received in revised form 14 August 2021; Accepted 16 August 2021
Available online 11 September 2021

Nomenclature

A	Inlet water flow in charge status (m^3/hr)
B	Inlet water temperature in charge status (°C)
C	Inlet water temperature in discharge status (°C)
N	Number of capsules
Q	Heat power of TES unit (kW)
V_b	Volume of a single paraffin wax capsule (m^3)
V_o	Space volume of the packed bed region (m^3)
CCD	Central composite design
HTF	Heat transfer fluid
mCHP	Micro combined heat and power
MEPCMs	Microencapsulated phase change materials
PCM	Phase change material
RSM	Response surface method
TES	Thermal energy storage

were studied using the spherical paraffin capsules during the melting and freezing processes. The results showed that the phase change period during the melting and freezing processes decrease even with decreasing the inlet temperature due to the Reynolds number increase, and the phase change of the capsule in the first layer is shorter than the seventh layer. Also, the phase change in the capsule center is longer than the capsule edge because the porosity at the edge of the reservoir is larger than that of the center. In recovering the heat of an outlet from a diesel engine using a heat exchanger and phase-change material, the heat exchanger efficiency was reported to be nearly 99% under all conditions at the end of the melting process. Nearly 10% to 15% of the total heat output is recovered by this system, with the maximum thermal capacity of the converter at full load and about 6.3 kW. The speed and efficiency of melting at higher loads are very high and are decreased with respect to the load [15]. Navarro et al. [16] investigated the PCM incorporation in a concrete core slab as a thermal storage and supply system. The main objective of this research project was to study the thermal performance of the slab and its components, in a theoretical analysis, as well as the suitability of the system in a Mediterranean continental climate. The result of this study has shown the concept was proved experimentally and compared to the theoretical results to demonstrate the potential of the technology. In another study, Weiguang et al. [17] investigated the Microencapsulated phase change materials (MEPCMs) on the efficiency of the energy storage systems. Particularly, this study was focused on numerically assessing the energy saving potential of a binary MEPCM drywall system which is capable of operating within two different phase change transitional temperature ranges. The simulation results demonstrated that the thermal energy charge time and thermal energy charge/discharge amount of the binary MEPCM drywall were significantly increased when the MEPCM thickness increased from 1 mm to 5 mm,

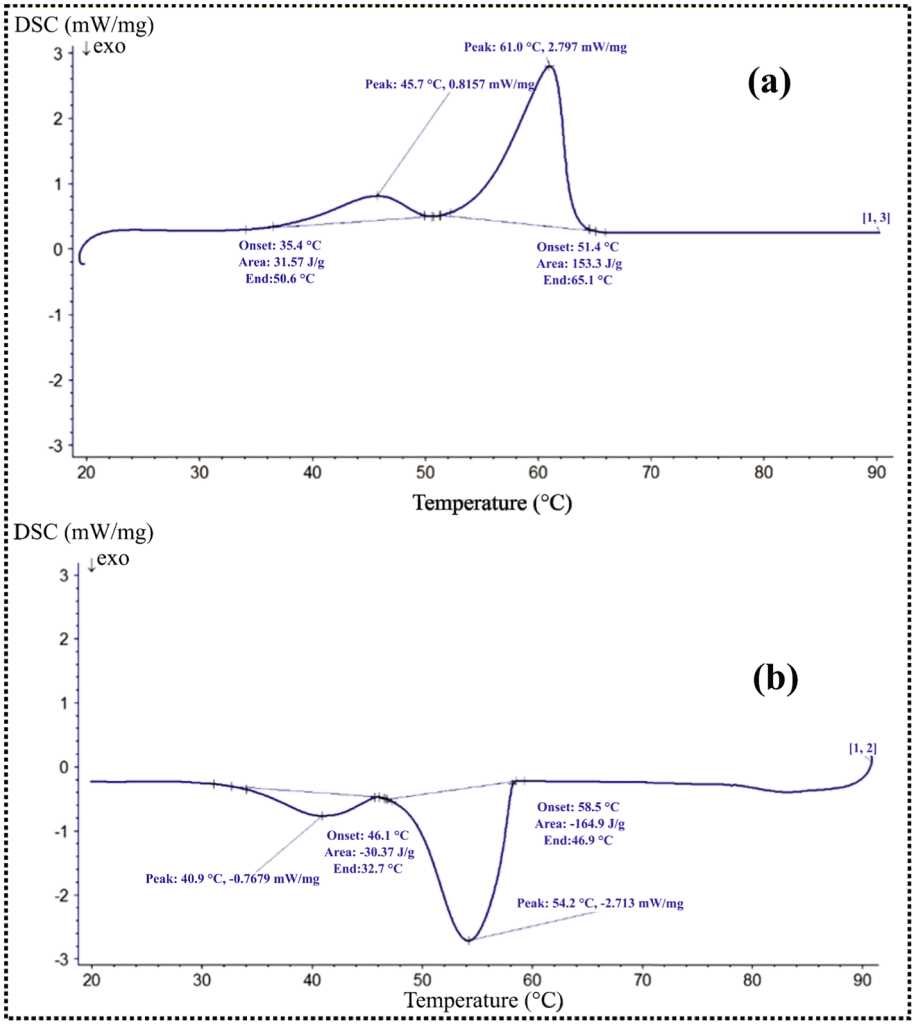

Fig. 1. (a) DSC diagram concerning the forward reaction of phase change material (melting); (b) DSC diagram of concerning the reverse reaction of phase change material (freezing).

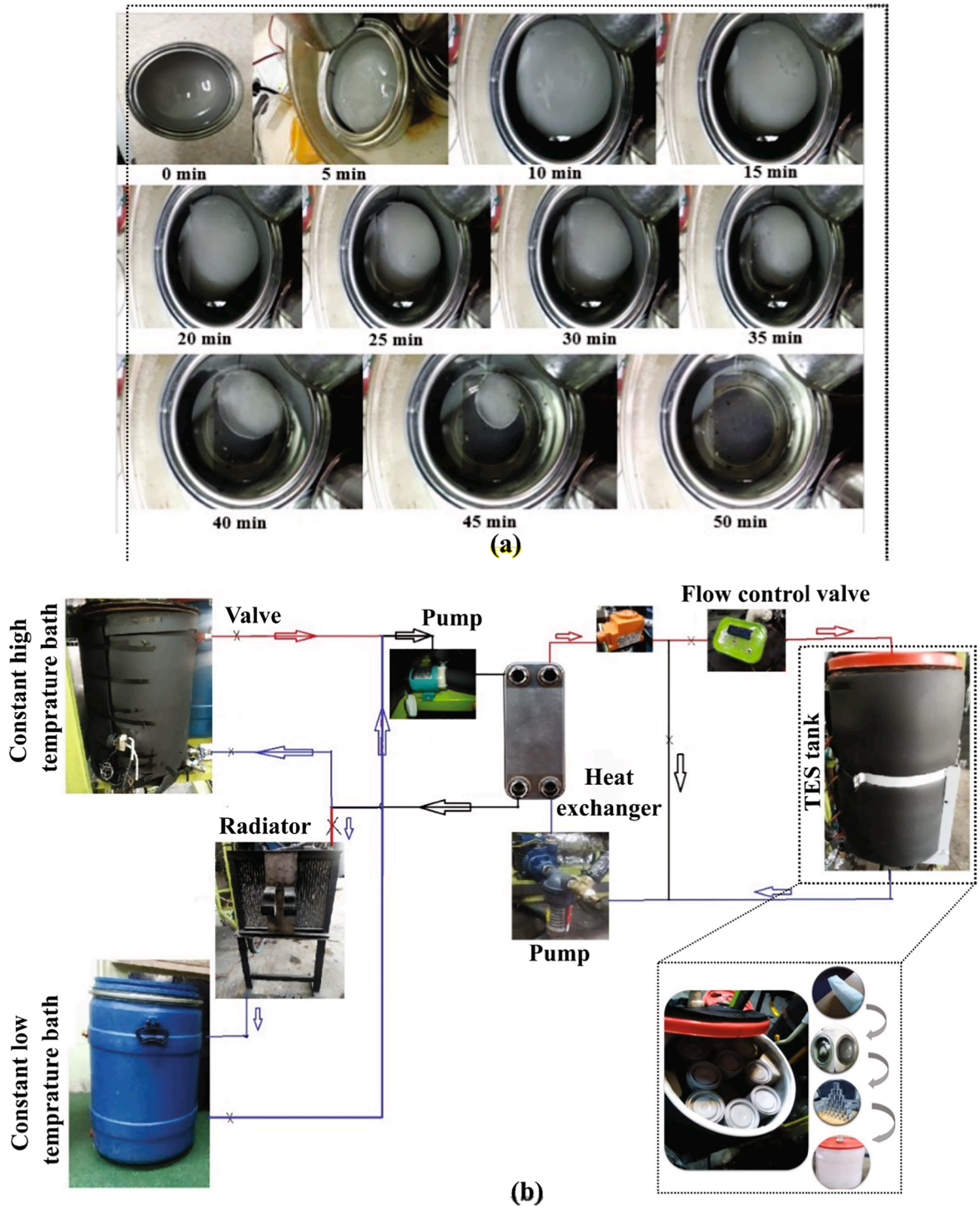

Fig. 2. Experimental Setup of TES system: (a) Melting process of the PCM during the time; (b) Experimental set-up for investigating the charging/discharging process TES system.

and the 5 mm thick layer had adequate capacity to balance the thermal energy during day and night. Weiguang et al. [18] in another research project tried to develop a new MEPCM for solar TES systems by encapsulation of paraffin wax with poly (urea formaldehyde). The differential scanning calorimetric analysis results showed that the melting temperatures were slightly increased by 0.14–0.72 °C after encapsulation. A thermogravimetric test showed that the sample weight decreased while the weight loss starting temperature was slightly increased after encapsulation. Finally, we can conclude that different studies have been done on application of PCM on improvement the efficiency of energy conversion/storage systems. Some of the application of the PCM in energy systems are as follows: PCM blind system for double skin façade integration [19,20], Microencapsulated PCM for solar thermal energy storage [21], Solidification inside a clean energy storage unit utilizing PCM with copper oxide nanoparticles [22], Experimental study and performance analysis on solar photovoltaic panel integrated with PCM [23], An innovative battery thermal management with thermally induced flexible PCM [24], Heat transfer inside cooling system based on PCM with alumina nanoparticles [25].

Based on the result of previous studies, we can conclude that the PCM

has an effective impact on the on efficiency of the energy storage systems. In particular, the PCM cylinder capsules inside the TES units have been found to outperform other types of capsules due to their higher contact surface with the heat transfer fluid. However, studies on the effect of the temperature and fluid properties of the fluid are used as heat transfer fluid (HTF) in charge and discharge status, on the performance of TES unit, are in the initial stage. It also seems necessary to include the storage capacity as well as charge and discharge times as further intact areas of investigation which fill the gap in the current research work. The major objective of the present study is to investigate the effect of heat transfer fluid (HTF) temperature range on the performance of the latent heat thermal energy storage system consisting of micro cylindrical capsules. The effects of inlet heat transfer fluid temperature and fluid flow rate have been discussed and optimized for charging and discharging processes.

Materials and methods

Material

The type of PCM was chosen based on the needed temperature range. Consequently, a material with the melting point of the same temperature range was chosen. The organic compounds and salt hydrates are among the materials with temperature ranges of 0–100 °C, and concerning the cost-effectiveness of organic compounds, the paraffin wax is used [12]. PCMs can be encapsulated in cylindrical, spherical, and cubic forms. In the current study, the cylindrical containers were used to encapsulate the PCM. The reason for the use of these containers was that they were made of the disposable iron cans which result in reduction of cost and help recycle these materials. In addition, compared to the common polyethylene encapsulation containers, the disposable iron containers have a higher conductivity coefficient which led to rapid melting and better heat transfer with the heat transfer fluid [26,27].

Material characterization

Using the Differential Scanning Calorimetry (DSC) test, it is feasible to obtain the melting point, glass transfer temperature, and crystalline percentage. The DSC test was performed using Maia DSC 200-F3 device and the melting as well as freezing curves were extracted (Fig. 1).

According to the Fig. 1, the paraffin wax was melted in the temperature range from 54 to 61 °C. The first and second peak points represent the crystallization temperature and melting temperature, respectively. Also, below the area of region is known as the released latent heat. Hence, in this study, the distance between the maximum point of two diagrams is considered as the melting range of the paraffin wax and the inlet temperatures of charge and discharge are chosen based on it.

Equipment and methods

The experimental setup used for thermal performance of TES system using latent heat and sensible heat of the PCMs (paraffin wax) is shown in Fig. 2. Investigations are carried out by integrating this storage system with the constant heat source. To meet the above requirement, a cylindrical tank of 40 L capacity with Φ320 × 485 mm dimensions is used. The storage tank is insulated with elastomeric insulation of 20 mm thick to prevent loss of heat. For measuring the temperature of HTF, thermocouples (Pt 100) were located along the axis of the tank at the locations of x/L = 0.25, 0.5, and 0.75 (x is the axial distance from the top of the TES tank in mm and L is length of the TES tank). Thermocouples with the standard accuracy of ±2.2C% or ±0.75% were also used for measuring the inlet and outlet temperatures of HTF. To determine the performance of the TES system, 36 cylindrical capsules PCM with the dimension of Φ93 × 100 mm were used.

In the present study, water mainly serves as the HTF while encapsulated paraffin wax is the primary TES material. Some physical properties of the paraffin wax used in this study are listed in Table 1. Each capsule was filled with 300 g of paraffin wax which is sealed with a lid and epoxy to avoid leakage. 36 capsules of paraffin wax were used to build the PCM packed bed, occupying 485 mm height of the main body. According to Eq. (1), the porosity of the packed bed, ε, calculated. After the calculation, the porosity of the packed bed obtained of 0.373.

Table 1
Physical properties of paraffin wax.

Property	value
Specific heat (solid phase)	1.97 kJ/(kg.K)
Specific heat (liquid phase)	2.1 kJ/(kg.K)
Density (solid phase)	0.866 kg/m^3
Density (liquid phase)	0.774 kg/m^3
Enthalpy of fusion	195.27 kJ/kg
Phase change temperature range	54.2–61 °C

Table 2
Theoretical heat storage capacity of 50 °C/80 °C case.

	Heat storage capacity (kJ)	Percentage
Water tank		
Total	5000.95	100%
PCM-water tank		
Latent heat of paraffin wax	2147.97	
Sensible heat of paraffin wax	529.91	
Sensible heat of water	2000.38	
Sensible heat of stainless-steel shell		
Total		100%

$$\varepsilon = 1 - \frac{NV_b}{V_o} \quad (1)$$

where N is the number of capsules, V_b and V_o are the volume of a single paraffin wax capsule and the space volume of the packed bed region (including the space between capsules), respectively.

The theoretical heat storage capacity of 50 °C/80 °C case is listed in Table 2. As shown in Table 2, in the operation condition of between 50 °C and 80 °C, the theoretical heat storage capacity is 130,365.23 kJ. Compared to the water TES tank operating under the same condition, the energy storage density is increased by 29.62%.

In the present study, different variables considered such as the HTF inlet temperature and the HTF flow rate. During the charging process, the HTF is circulated through the TES tank continuously. Initially, temperature of PCM capsule is 32 °C and as the HTF exchanges its heat energy to PCM, the PCM is heated up to melting temperature. Later, heat is stored as the latent heat once the PCM melts and becomes liquid. The energy is then stored as the sensible heat in liquid PCM. Temperature of the PCM and HTF are recorded at 1 min's intervals.

Experimental design and optimization process

When many factors and interactions affect desired responses, response surface methodology (RSM) is an efficient tool for optimizing the process. The RSM is a set of statistical and mathematical techniques used for modelling, and analyzing experiments [28]. The advantage of using RSM is that it reduces the number of experiments required and for use in industrial projects and has economic benefits [29]. One of the important goals of RSM is to determine the relationship between one or more response variables and several independent variables in multi-objective experiments [30].In the present study, Design-Expert® Software (Version 10.) [31] was employed for statistical analysis, and optimization was performed using RSM to achieve the highest thermal power of TES unit and highest thermal performance of TES unit. Central Composite Design (CCD) with three factors was used to evaluate the

Table 3
Dependent and independent variables of experiment matrix in response level method.

	Chosen levels								
Independent variables	1			0			−1		
Charging flow (lit/hr)	660			480			300		
Charging temperature °C	75			70			65		
Discharging temperature °C	45	40	35	45	40	35	45	40	35
Dependent variables									
Thermal power of TES unit									
Thermal performance of TES unit									

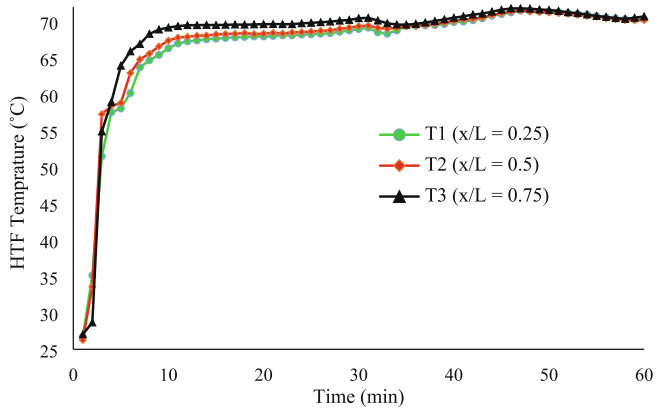

Fig. 3. Temperature distribution (in line with tank length) with temperature and constant inlet flow (T_{in} = 70 °C, Q_{in} = 480 L/h).

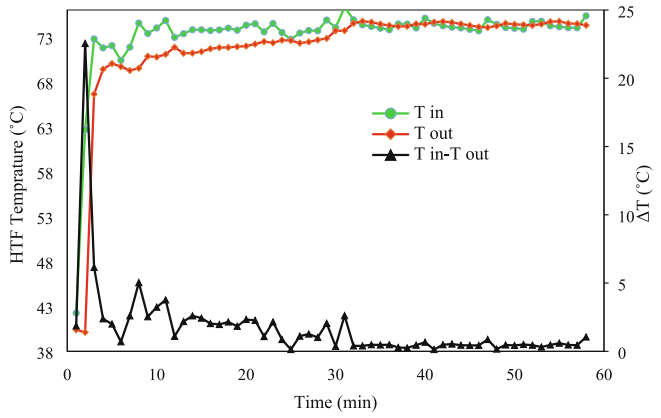

Fig. 4. Thermal variations of HTF and ΔT during time (T_{in} = 70 °C, Q_{in} = 480 L/h).

effects of these factors on dependent variables. CCD has three levels for each factor (−1, 0, and 1). The encoded and actual levels of the independent variables for designing experiments with CCD are presented in Table 3.

Results and discussion

Results of TES unit evaluation

Fig. 3 represents the thermal variations of HTF in line during the TES tank length (x/L = 0.25, 0.5, 0.75) in the operation condition of 70 °C inlet temperature and 480 L/h volumetric flow. Based on the result, water temperature in all layers increases quickly until reaching the PCM melting temperature. However, HTF temperature increase in the location of x/L = 0.25 of the tank is faster since the hot water flows in the tank entry. In this layer, the temperature reaches at 70 °C in 7 min, and then continues constant to the extent in which PCM is melted completely. As shown in Fig. 4, there is the same direction in the layers. This is because after the PCM is completely melted in the first layer, the absorbed heat decreases due to the reduction of the local temperature difference between PCM and HTF in the first layer. Therefore, heat transfer as well as temperature increase in the second layer. It was also observed that the temperature changes of the tank layers are uniform and this temperature uniformity is due to the presence of PCM metal containers as well as metal punches inside the storage tank that transfer heat through conduction in the radial direction of the tank. Therefore, an almost uniform temperature was observed throughout the storage tank.

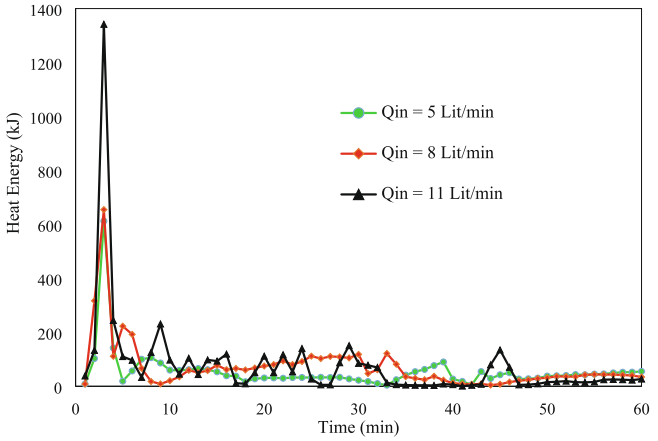

Fig. 5. Stored heat energy throughout the PCM charging process concerning different HTF flows (T_{in} = 75 °C).

Fig. 4 illustrates the thermal variations of HTF and ΔT during time for the inlet temperature variations (T_{in}), outlet temperature (T_{out}), and temperature difference (T_{in} − T_{out}) in the case of PCM tank charging process at 70 °C and 480 L/h inlet flow. Inlet and outlet temperatures are increased by time ΔT value increases by 23 °C in the initial five minutes and follows a decreasing trend afterwards since PCM is heated by the melting temperature and absorbs considerable latent heat. Fig. 5 shows the stored heat energy throughout the PCM charging process concerning different HTF flows. According to the result, the heat energy in the beginning of charging increase and follows a decreasing trend afterwards. Such a thermal drop is due to the decrease of temperature difference between the HTF and storage tank. Furthermore, PCM is absorbed following the charging process and the stored heat energy is almost uniform due to the uniform thermal difference between HTF and the storage tank.

Results of statistical analyses

The experimental runs of the independent variables with CCD design and experimental results are given in Table 4. As shown in Table 3, independent parameters include the inlet water flow in charging process (A), inlet water temperature in charging process (B), and inlet water temperature in discharging status (C). Also, dependent parameters (results) include the heat power level (Q) and TES unit thermal performance (N_t). Based on these results, maximum heat power and maximum thermal performance of PCM thermal tank, which are 1.74 kW and 97.2%, pertain to experiment 8 with 75 °C charging inlet temperature, 660 Lit/hr charging flow, and 35 °C discharging inlet temperature. In

Table 4
Data derived from different experiments based on the CCD experiment design.

Independent Parameters				Dependent Parameters	
Experiment	Inlet water flow in charge status (Lit/hr) A	Inlet water temperature in charge status (°C) B	Inlet water temperature in discharge status (°C) C	Heat power of TES unit (kW) Q	Thermal performance of TES unit (%) N_t
1	660	65	35	0.6	34.6
2	300	75	35	1.17	70.7
3	480	70	45	0.66	37.0
4	660	70	45	0.84	52.1
5	480	70	45	0.68	42.0
6	480	70	40	0.77	42.8
7	660	75	40	1.61	87.9
8	660	75	35	1.14	97.2
9	300	75	40	1.06	64.7
10	660	70	40	0.96	55.9
11	300	65	35	0.41	25.4
12	480	65	35	0.51	29.1
13	480	65	40	0.38	22.8
14	660	75	45	1.51	94.3
15	480	70	35	0.87	48.4
16	480	70	40	0.75	47.4
17	480	70	40	0.81	48.1
18	480	70	45	0.68	41.4
19	480	70	35	0.95	52.0
20	300	65	45	0.31	18.9
21	480	70	35	0.86	48.9
22	660	70	35	1.05	64.1
23	660	65	40	0.53	58.7
24	660	65	45	0.42	24.3
25	480	70	45	0.66	39.3
26	480	65	45	0.42	23.4
27	300	75	45	1.01	61.0
28	480	75	35	1.52	78.6
29	480	75	40	1.46	86.6
30	300	65	40	0.37	19.3
31	300	70	45	0.56	35.0
32	480	75	45	1.24	91.5
33	300	70	35	0.68	37.6
34	480	70	35	0.94	49.7
35	480	70	40	0.78	50.4
36	300	70	40	0.70	45.2

Table 5
The results of analysis of variance (ANOVA) concerning the level of heat power produced by PCM thermal tank.

Source of change	Degree of freedom	Sum of squares	F value	p-value
Model	11	4.85	268.28	0.0001^{**}
A	1	0.50	302.03	0.0001^{**}
B	1	3.89	2366.79	0.0001^{**}
C	2	0.22	67.03	0.0001^{**}
AB	1	0.11	68.19	0.0001^{**}
AC	2	0.004978	1.51	0.0001^{**}
BC	2	0.008400	2.55	0.2404^{ns}
A^2	1	0.0003556	0.22	0.0987^{ns}
B^2	1	0.11	66.22	0.6461^{ns}
Residual	24	0.039	–	0.0001^{**}
Lack of Fit	15	0.031	2.14	–
Error	9	0.008650	–	0.1257^{ns}
Total	35	4.89	–	–

ns = not significant.
** = Very significant P value ≤ 0.01.

Table 6
The results of analysis of variance (ANOVA) concerning the thermal performance of PCM thermal tank.

Source of change	Degree of freedom	Sum of squares	F value	p-value
Model	17	0.043	81.71	0.0001^{**}
A	1	0.0032	104.86	0.0001^{**}
B	1	0.036	1183.66	0.0001^{**}
C	2	1.232×10^{-3}	20.12	0.0001^{**}
AB	1	1.099×10^{-4}	3.59	0.0743^{ns}
AC	2	1.080 × 10–5	0.18	0.8397^{ns}
BC	2	6.781×10^{-4}	11.02	0.0007^{**}
A^2	1	2.319×10^{-6}	0.076	0.0002^{**}
B^2	1	6.413×10^{-4}	20.94	0.4143^{ns}
ABC	2	5.671×10^{-5}	0.93	0.7055^{ns}
A^2C	2	2.178×10^{-5}	0.36	0.0480*
B^2C	2	2.212×10^{-4}	3.61	
Residual	18	8.755×10^{-3}		
Lack of Fit	9	7.205×10^{-3}	2.56	0.0891^{ns}
Error	9	1.550×10^{-3}		
Total	35	0.44		

ns = not significant.
** = Very significant P value ≤ 0.01.

contrast, the minimum heat power level and tank thermal performance, which are 0.31 kW and 18.9%, pertain to the experiment 20 with 65 °C charging inlet temperature, 300 L/h inlet flow, and 45 °C discharging inlet temperature.

Heat power of TES unit

Table 6 shows the results of variance analysis concerning the level of produced heat power of TES unit. The effect of inlet flow in charging status is significant at 1% probability level while the square of this factor is not significant. Also, the effect of inlet temperature and square of this factor are significant at 1% probability level. The effect of inlet temperature factor in discharging condition was examined as a categoric factor which was found to be significant at 1% probability. Of the

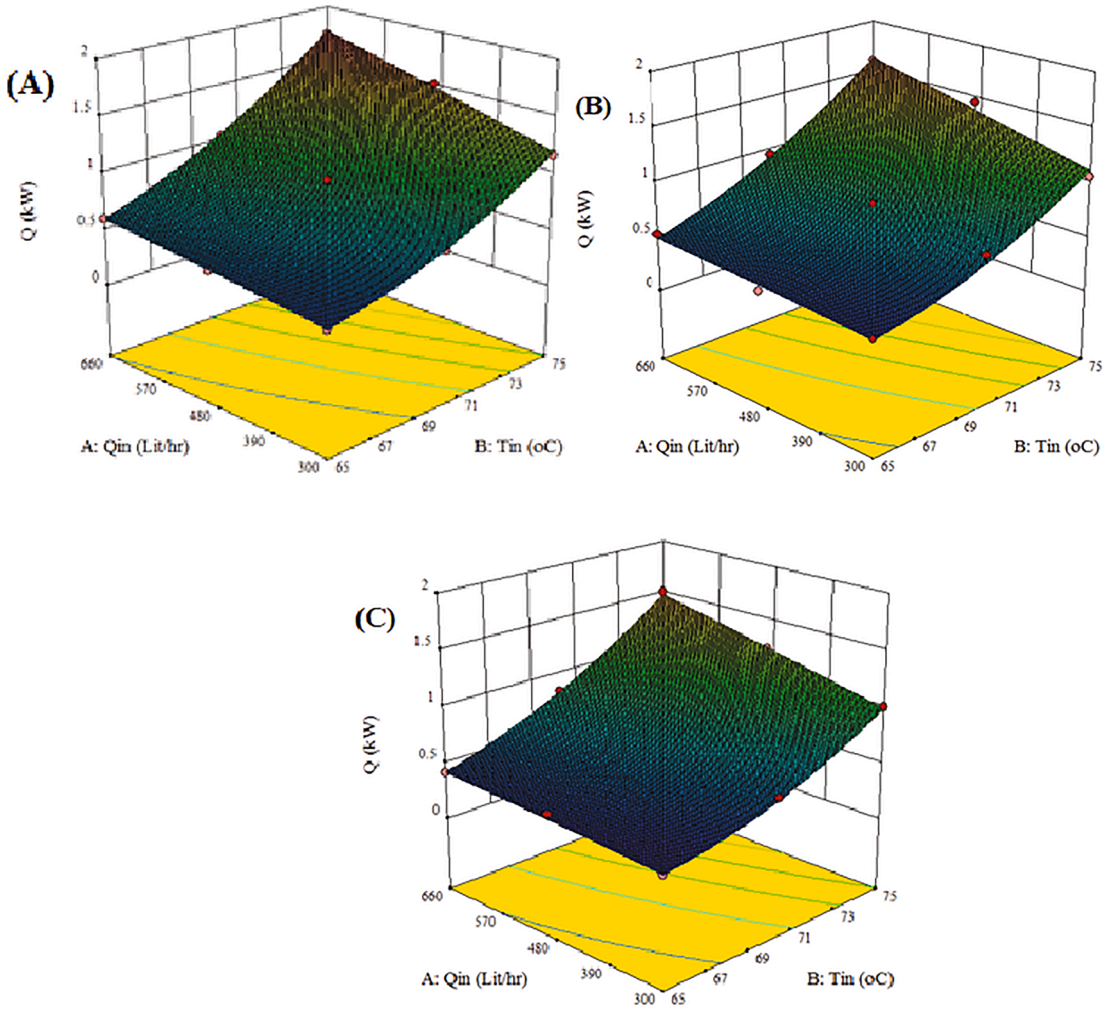

Fig. 7. 3D surface diagram concerning the interactive effect of temperature and inlet water flow (A) at 35 °C discharge constant temperature; (B) at 40 °C discharge constant temperature; (C) at 45 °C discharge temperature on heat power level of TES unit.

interactive effects, the interactive effect of temperature and charge flow have been reported to be significant at 1% probability. Considering the sum of squares (3.89), the inlet temperature factor in charging status has the maximum variations in data derived from the heat power level produced by TES unit and has the highest effect on increasing the performance of TES unit.

The response surface methodology has suggested the quadratic model with R-squared of 0.98 for the heat power dependent variable. According to Table 5, the analysis of variance concerning the quadratic equation for the level of produced power was significant at 1% level which represents the efficiency of obtained model. One of the considerable criteria in response surface methodology is the lack of fit index. In case this index is significant, responses are predicted by the model with a weak probability. As Table 5 illustrates, the lack of fit index is not significant for the produced power level, thus the quadratic model is of sufficient accuracy for estimating the data. Having excluded non-significant coefficients, the quadratic model was obtained based on real factors and different discharge temperatures which is shown in Eqs. (3)–(5) as follows:

35 °C discharge temperature:

$$\dot{Q} = 20.02 - 0.0063 \times A - 0.61 \times B + 1.074 \times AB - 2.06 \times 10^{-7} \times A^2 + 0.0047 \times B^2 \quad (3)$$

45 °C discharge temperature:

$$\dot{Q} = 20.14 - 0.0064 \times A - 0.61 \times B + 0.00011 \times AB - 2.06 \times 10^{-7} \times A^2 + 0.0047 \times B^2 \quad (4)$$

45 °C discharge temperature:

$$\dot{Q} = 20.64 - 0.0065 \times A - 0.62 \times B + 0.00011 \times AB - 2.06 \times 10^{-7} \times A^2 + 0.0047 \times B^2 \quad (5)$$

In these equations, $\dot{Q}$ is the heat power level produced by TES unit, A is the charge inlet flow level, and B is the charge inlet temperature. The positive mark of estimated regression coefficients derived from the central mixed model indicates direct effect of independent variables on response variables, and the negative mark emphasizes indirect effect of independent variable on response variables. Therefore, as the above-mentioned equations represent, the effect of charge inlet temperature on heat power level of TES unit is higher than the effect of inlet flow. Fig. 7 shows the three-dimensional diagram concerning the interactive effect of factors examined in this study based on the heat power of TES unit. The maximum and minimum heat power of TES unit pertain to the temperatures and inlet flows of 75 °C, 660 L/h, and 65 °C , 300 L/h, respectively. The heat power level for aforementioned temperature and flow at 35 °C is 1.74, 0.41 kW, at 40 °C is 1.61, 0.37 kW, and at 45 °C is 1.51, 0.311 kW, respectively. Hence, according to the obtained results,

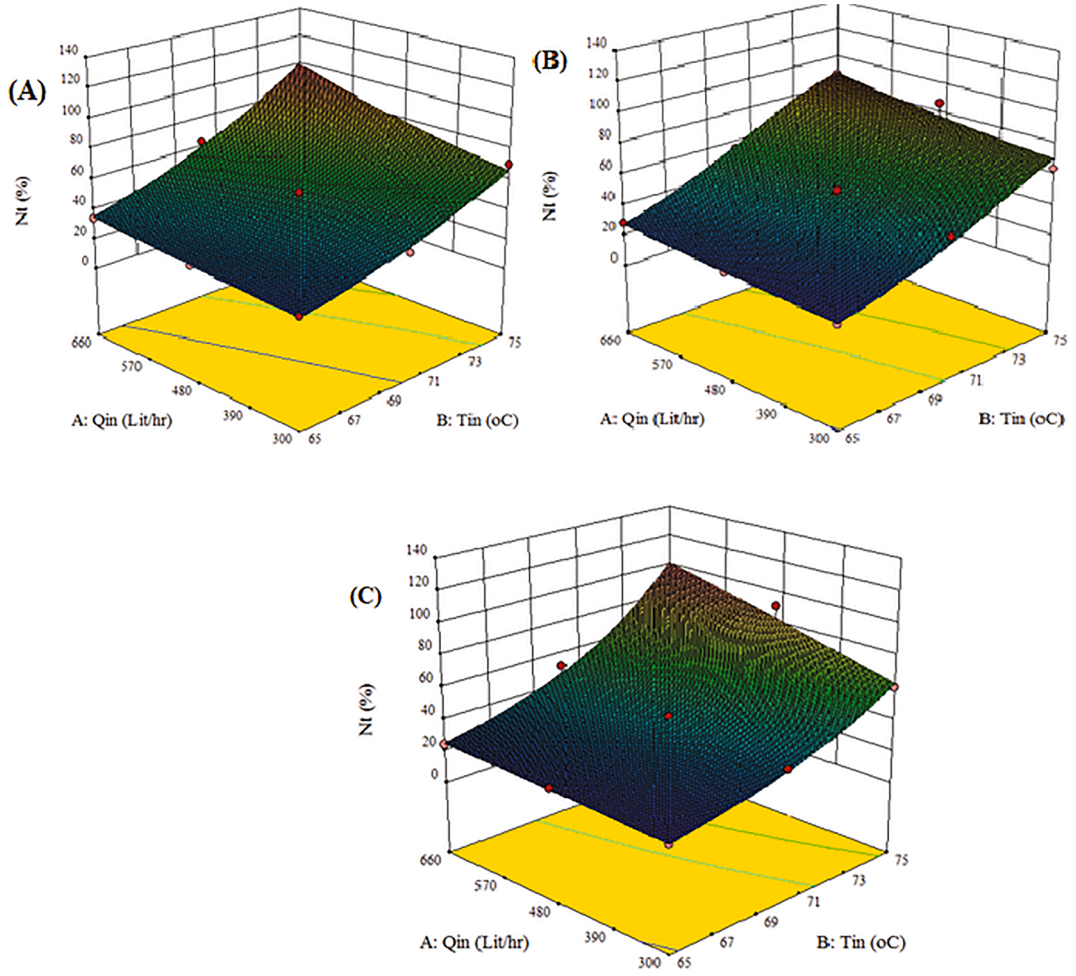

Fig. 8. 3D Surface diagram concerning the interactive effect of temperature and inlet water flow (a) at 35 °C discharge constant temperature; (b) at 40 °C discharge constant temperature; (c) at 45 °C discharge temperature on thermal performance level of TES unit.

maximum heat power pertains to 75 °C inlet temperature, 660 L/h inlet flow, and 35 °C discharge temperature. Also, minimum heat power is related to 65 °C inlet temperature, 300 L/h inlet flow, and 45 °C discharge temperature. Consequently, maximum heat power of TES unit occurs at higher temperature and flow and at lower discharge temperature.

Thermal performance of TES unit

Table 6 shows the results of variance analysis concerning the level of produced thermal performance of TES unit. The effect of inlet flow in charging status is significant at 1% probability level while the square of this factor is not significant. Also, the effect of inlet temperature and square of this factor are significant at 1% probability level. The effect of inlet temperature factor in discharging condition was examined as a categoric factor which was found to be significant at 1% probability. The inlet temperature factor in charging status has the maximum variations in data derived from the heat power level produced by TES unit and has the highest effect on increasing the performance of TES unit.

The response surface methodology has suggested the quadratic model with 0.92 R-squared for the thermal performance dependent variable. According to Table 6, the analysis of variance concerning the quadratic equation for the thermal performance was significant at 1% level which represents the efficiency of obtained model. One of the considerable criteria in response surface methodology is the lack of fit index. As Table 6 illustrates, the lack of fit index is not significant for the thermal performance level, thus the quadratic model is of sufficient accuracy for estimating the data. Having excluded non-significant coefficients, the quadratic model was obtained based on real factors and different discharge temperatures which is shown in Eqs. (3)–(5) as follows:

35 °C discharge temperature:

$$\frac{1}{\sqrt{N_t}} = 1.92358 - 2.77913 \times 10^{-4} \times A - 0.041162 \times B + 3.03174 \times 10^{-6} \times AB + 1.26801 \times 10^{-8} \times A^2 + 2.31616 \times 10^{-4} \times B^2 \quad (6)$$

40 °C discharge temperature:

$$\frac{1}{\sqrt{N_t}} = 4.26180 - 4.96555 \times 10^{-4} \times A - 0.10425 \times B + 6.47261 \times 10^{-6} \times AB + 2.57174 \times 10^{-8} \times A^2 + 6.54558 \times 10^{-3} \times B^2 \quad (7)$$

45 °C discharge temperature:

$$\frac{1}{\sqrt{N_t}} = 1.86446 - 2.02188 \times 10^{-4} \times A - 0.036769 \times B + 5.84082 \times 10^{-7} \times AB + 8.82496 \times 10^{-8} \times A^2 + 1.88241 \times 10^{-4} \times B^2 \quad (8)$$

In these equations, N_t is the thermal performance level of TES unit, A is the charge inlet flow level, and B is the charge inlet temperature. As

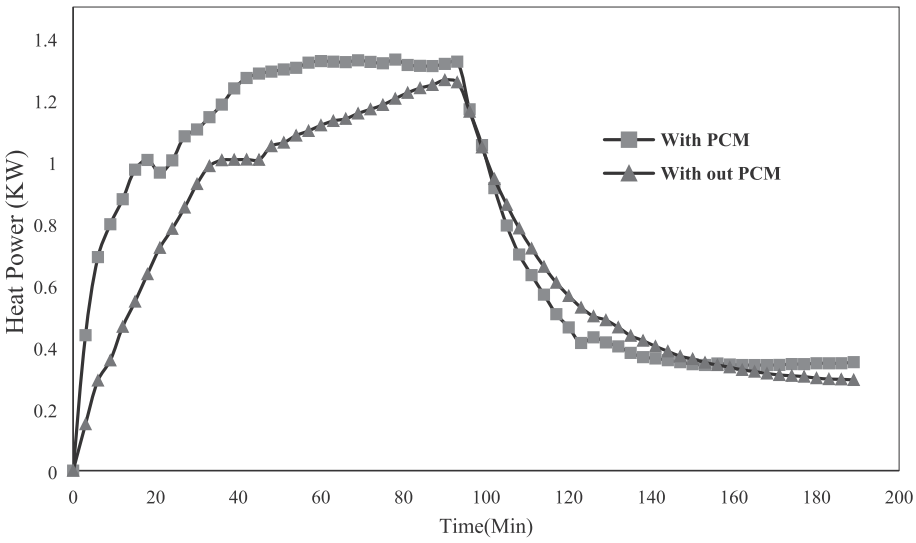

Fig. 9. The storage heat power level in the second layer in the presence and absence of PCM.

the above-mentioned equations represent, the effect of charge inlet temperature on thermal performance level of TES unit is higher than the effect of inlet flow. Fig. 8 shows the three-dimensional diagram concerning the interactive effect of each factor in different discharge temperatures.

Similar to the heat power variable, maximum thermal performance is achieved when the temperature and charge inlet flow are at the maximum level and discharge temperature is at the minimum level. Thus, as it is clear, the increase of charge inlet temperature from 65 °C to 75 °C in 480 L/h constant inlet flow and 40 °C discharge inlet temperature results in increase of thermal performance level from 22.8% to 86.6%. Under the same condition, 660 L/h, and 40 °C discharge inlet temperature, the aforementioned level reaches 28.7% to 87.9% which represents higher effect of inlet temperature factor on the thermal performance of TES unit when compared to the effect of inlet flow.

Performance of TES with PCM and without PCM

Studies were conducted to compare the performance of heat storage tank with PCM and without PCM. Therefore, experiments were carried out for both storing dimensions at equal temperature and inlet. The experiment was run at 75 °C inlet temperature, 450 L/h inlet flow, and 40 °C discharge temperature. According to Fig. 9, the heat power level in the second layer in the presence of PCM under the same time condition is higher than the case of storage with without PCM.

Optimization using RSM

The optimal value for each of the studied variables was predicted using Eqs. (3)–(8) in order to obtain the highest thermal power of TES unit and highest thermal performance of TES unit. This Eqs are based on a regression polynomial equation, which is derived from the RSM model. The optimal value for each of the variables is as follows: the charging inlet temperature of 75 °C, charging inlet flow of 1.8^{-4} m^3/s, and discharging inlet temperature of 35 °C. The regression polynomial equation predicts that if the variables are set to these values, the highest the maximum thermal performance of 96.4% and the maximum heat power level of 1.7 kW can be achieved. In order to verify this prediction, the optimized points were evaluated experimentally under three replications. The average heat and thermal performances of TES unit were obtained as 1.65 kW and 95%. Thus, the experimental results show that the value predicted by RSM is in excellent agreement with the experimental measurements.

Conclusions

The present study investigated the thermal behavior of cylindrical modules in a thermal energy storage (TES) unit as a combined sensible and latent heat. The response surface methodology (RSM) approach was used for multi-objective optimization of the different variables (inlet water flow in charge status (Lit/hr), inlet water temperature in charge status (°C), and inlet water temperature in discharge status(°C) in order to maximize the heat power of TES unit (kW) and thermal performance of TES unit (%). Followings are the results drawn from the present study:

- Similar to the charge temperature factor, the increase of charge inlet flow (at charge and discharge constant inlet temperatures) leads to the increase of output variables, however such an extent is lower when compared to the effect of charge inlet temperature.
- Considering that the tank charge time in the presence of PCM, based on the quality of using this material in heat storing tank, is equal to the case of PCM absence, the application of such types of tanks to store the heat is justifiable as they outperform the cases with the PCM absence.
- Maximum heat power and maximum thermal performance of PCM thermal tank, which are 1.74 kW and 97.2%, pertain to 75 °C charging inlet temperature, 660 L/h charging flow, and 35 °C discharging inlet temperature. In addition, the minimum heat power level and thermal performance, which are 0.31 kW and 18.9%, pertain to 65 °C charging inlet temperature, 300 L/h inlet flow, and 45 °C discharging inlet temperature.
- 75 °C charging inlet temperature, 660 L/hcharging inlet flow, and 35 °C discharging inlet temperature is the most optimized condition for attaining the maximum thermal performance (96.4%), and that the maximum heat power level is 1.7 kW.

Declaration of Competing Interest

The authors declare that they have no known competing financial interests or personal relationships that could have appeared to influence the work reported in this paper.

Acknowledgement

The authors are grateful to Tarbiat Modares University (http://www.modares.ac.ir) for financial supports given under IG/39705 grant for Renewable Energies of Modares research group.

References

[1] Kensby J, Trüschel A, Dalenbäck J-O. Potential of residential buildings as thermal energy storage in district heating systems–results from a pilot test. Appl Energy 2015;137:773–81.

[2] Yusaf T, Hamawand I, Baker P, Najafi G. The effect of methanol-diesel blended ratio on ci engine performance. Int J Autom Mech Eng 2013;8:1385–95.

[3] Oró E, Miró L, Farid MM, Martin V, Cabeza LF. Energy management and CO2 mitigation using phase change materials (PCM) for thermal energy storage (TES) in cold storage and transport. Int J Refrig 2014;42:26–35.

[4] Ettefaghi E, Ghobadian B, Rashidi A, Najafi G, Khoshtaghaza MH, Rashtchi M, et al. A novel bio-nano emulsion fuel based on biodegradable nanoparticles to improve diesel engines performance and reduce exhaust emissions. Renewable Energy 2018;125:64–72.

[5] Iverson BD, Conboy TM, Pasch JJ, Kruizenga AM. Supercritical CO2 Brayton cycles for solar-thermal energy. Appl Energy 2013;111:957–70.

[6] Navarro L, De Gracia A, Colclough S, Browne M, McCormack SJ, Griffiths P, et al. Thermal energy storage in building integrated thermal systems: a review. Part 1. active storage systems. Renewable Energy 2016;88:526–47.

[7] Cabeza L, Martorell I, Miró L, Fernández A, Barreneche C. Introduction to thermal energy storage (TES) systems. In: Advances in Thermal Energy Storage Systems. Elsevier; 2015. p. 1–28.

[8] Najafi G, Ghobadian B, Yusaf TF, Rahimi H. Combustion analysis of a CI engine performance using waste cooking biodiesel fuel with an artificial neural network aid. Am J Appl Sci 2007;4(10):759–67.

[9] Abdolbaqi MK, Azmi WH, Mamat R, Mohamed NMZN, Najafi G. Experimental investigation of turbulent heat transfer by counter and co-swirling flow in a flat tube fitted with twin twisted tapes. Int Commun Heat Mass Transfer 2016;75:295–302.

[10] Heier J, Bales C, Martin V. Combining thermal energy storage with buildings – a review. Renewable Sustainable Energy Rev 2015;42:1305–25.

[11] Najafi G, Ghobadian B. LLK1694-wind energy resources and development in Iran. Renewable Sustainable Energy Rev 2011;15(6):2719–28.

[12] Su W, Darkwa Jo, Kokogiannakis G. Review of solid–liquid phase change materials and their encapsulation technologies. Renewable Sustainable Energy Rev 2015;48:373–91.

[13] Yazdanshenas E, Asgari F, Babol Mazandaran I, Yazdanshenas E. Experimental Investigation of a Solar LiCl Dryer System.

[14] Cho K, Choi SH. Thermal characteristics of paraffin in a spherical capsule during freezing and melting processes. Int J Heat Mass Transfer 2000;43(17):3183–96.

[15] Pandiyarajan V, Chinna Pandian M, Malan E, Velraj R, Seeniraj RV. Experimental investigation on heat recovery from diesel engine exhaust using finned shell and tube heat exchanger and thermal storage system. Appl Energy 2011;88(1):77–87.

[16] Navarro L, de Gracia A, Castell A, Álvarez S, Cabeza LF. PCM incorporation in a concrete core slab as a thermal storage and supply system: proof of concept. Energy Build 2015;103:70–82.

[17] Su W, Darkwa J, Kokogiannakis G. Numerical thermal evaluation of laminated binary microencapsulated phase change material drywall systems. Build Simul 2020;13:89–98.

[18] Su W, Li Y, Zhou T, Darkwa J, Kokogiannakis G, Li Z. Microencapsulation of paraffin with poly (urea methacrylate) shell for solar water heater. .Energies 2019;12(18):3406.

[19] Li Y, Darkwa Jo, Kokogiannakis G, Su W. Phase change material blind system for double skin façade integration: system development and thermal performance evaluation. Appl Energy 2019;252:113376.

[20] Li Y, Darkwa J, Kokogiannakis G, Wjijol Su. Effect of design parameters on thermal performance of integrated phase change material blind system for double skin façade buildings. Low Carbon Technol 2019;14(2):286–93.

[21] Su W, Darkwa Jo, Kokogiannakis G. Development of microencapsulated phase change material for solar thermal energy storage. Appl Therm Eng 2017;112:1205–12.

[22] Ma X, Sheikholeslami M, Jafaryar M, Shafee A, Nguyen-Thoi T, Li Z. Solidification inside a clean energy storage unit utilizing phase change material with copper oxide nanoparticles. J Clean Prod 2020;245:118888.

[23] Li Z, Ma T, Zhao J, Song A, Cheng Y. Experimental study and performance analysis on solar photovoltaic panel integrated with phase change material. Energy 2019;178:471–86.

[24] Wu W, Liu J, Liu M, Rao Z, Deng H, Wang Q, et al. An innovative battery thermal management with thermally induced flexible phase change material. Energy Convers Manag 2020;221:113145.

[25] Bondareva NS, Buonomo B, Manca O, Sheremet MA. Heat transfer inside cooling system based on phase change material with alumina nanoparticles. Appl Therm Eng 2018;144:972–81.

[26] Zivkovic B, Fujii I. An analysis of isothermal phase change of phase change material within rectangular and cylindrical containers. Solar Energy 2001;70(1):51–61.

[27] Bilir L, İlken Z. Total solidification time of a liquid phase change material enclosed in cylindrical/spherical containers. Appl Therm Eng 2005;25(10):1488–502.

[28] Box GEP, Wilson KB. On the experimental attainment of optimum conditions. J R Stat Soc. Ser B (Methodological) 1951;13(1):1–38.

[29] Wang S, Chen F, Wu J, Wang Z, Liao X, Hu X. Optimization of pectin extraction assisted by microwave from apple pomace using response surface methodology. J Food Eng 2007;78(2):693–700.

[30] Almasi S, Ghobadian B, Najafi G, Dehghani Soufi M. A novel approach for bio-lubricant production from rapeseed oil-based biodiesel using ultrasound irradiation: multi-objective optimization. Sustainable Energy Technol Assess 2021;43:100960.

[31] Bezerra MA, Santelli RE, Oliveira EP, Villar LS, Escaleira LA. Response surface methodology (RSM) as a tool for optimization in analytical chemistry. Talanta 2008;76(5):965–77.